Microperoxidase-11 functionalized electrodes: an active monolayer interface for the electrocatalyzed reduction of Co^{II}–protoporphyrin IX reconstituted myoglobin and for the generation of integrated protein electrodes for bioelectrocatalyzed hydrogenation of acetylenes

Vered Heleg-Shabtai, Eugenii Katz, Shlomo Levi and Itamar Willner *

Institute of Chemistry and Farkas Center for Light-Induced Processes, The Hebrew University of Jerusalem, Jerusalem 91904, Israel

Microperoxidase-11, MP-11, is assembled as a monolayer on an Au electrode. The resulting MP-11 monolayer electrode mediates the electrocatalyzed reduction of Co^{II}–protoporphyrin IX reconstituted myoglobin, Co^{II}–Mb. The electrocatalyzed reduction of Co^{II}–Mb proceeds *via* the formation of a complex between the MP-11 monolayer and Co^{II}–Mb. The association constant of the complex formed between MP-11 and Co^{II}–Mb is $K_a = 1.6 \times 10^5$ M^{-1}. Cross-linking of the complex formed between Co^{II}–Mb and the MP-11 monolayer with glutaric dialdehyde yields a stable integrated electrocatalytic electrode for the stereospecific hydrogenation of acetylenedicarboxylic acid to maleic acid (current yield is *ca.* 80%). The electrocatalyzed hydrogenation of acetylenedicarboxylic acid reveals an isotope effect, $k_H/k_D \approx 2.7$, suggesting the insertion of the substrate to a Co^{III}–H species in the rate-limiting step of the hydrogenation process.

Introduction

Cytochrome c, cyt. c, acts as an electron transfer mediator for many redox proteins (or enzymes). The formation of organized inter-protein complexes is the key process for the cyt. c mediated reactions.[1,2] Microperoxidase-11, MP-11, is a heme-containing 11-amino acid oligopeptide that consists of the active site microenvironment of cyt. c.[3] Hemoproteins usually lack direct electrical contact with electrode surfaces, but the electron transfer communication is often stimulated by the appropriate modification of the electrode supports. Cytochrome c exhibits quasi-reversible redox features at bare glassy carbon[4] and In_2O_3 electrodes,[5] but shows reversible redox processes at Ag, Au, Pt electrodes modified by promoter groups[6] such as pyridine,[7] iodide,[8] thiophene[9] or imidazole.[10] Also, negatively charged monolayers associated with electrodes appropriately align cyt. c on electrodes and induce reversible electron transfer.[11] Other hemoproteins such as myoglobin, Mb, or hemoglobin, Hb, show usually an irreversible heterogeneous electron transfer at bare metallic electrodes[12] but hydrophilic In_2O_3 stimulates quasi-reversible electron transfer to myoglobin.[13] Thin films of Mb assembled onto pyrolytic graphite or In_2O_3 by the deposition of surfactant-based Mb-microemulsions yield quasi-reversible electrochemistry of the hemoprotein.[14] Also, promoter-modified electrodes, *i.e.* a benzimidazole-functionalized Ag electrode, enhance the interfacial electron transfer of Mb.[15] Mediated electrical contact of hemoproteins, *i.e.* Hb, was reported in the presence of diffusional redox dyes such as cresol blue, thionine or methylene blue.[16] Recently we have shown that a microperoxidase-11, MP-11, modified electrode mediates the electro-reduction of hemoprotein, *i.e.* cyt. c, Hb and Mb.[17]

Reconstitution of apo-hemoproteins with synthetic metal-porphyrin analogs yields semi-synthetic proteins of novel photochemical[18] and catalytic properties. For example, reconstitution of apo-myoglobin, apo-α- or apo-β-hemoglobin with Co^{II}–protoporphyrin IX, and subsequent substitution of the resulting proteins with a chromophore generated photoenzyme capable of photocatalyzing the hydrogenation of acetylenes[19] or CO_2-fixation.[20] Recently we reported in a preliminary note on the assembly of an integrated Co^{II}–protoporphyrin IX-reconstituted myoglobin/MP-11 electrode.[21] In this study we demonstrated that MP-11 mediates the electrocatalyzed reduction of Co^{II}-reconstituted Mb and this stimulates the hydrogenation of acetylenedicarboxylic acid.

The assembly of the integrated electrocatalytic electrode follows a general concept that was developed by our laboratory. That is, reconstitution of an apo-enzyme on a flavin monolayer-modified electrode surface,[22] or the temporary binding of an enzyme to an $NAD(P)^+$-monolayer, by affinity associative interactions, followed by cross-linking of the enzyme layer[23] yield integrated, electrically-contacted electrodes. In the present study we provide a comprehensive account of the organization of an integrated Co^{II}-reconstituted myoglobin, Co^{II}–Mb and MP-11 electrode, and the mechanistic features accompanying the electrocatalytic properties of the resulting electrode.

Experimental

Materials

Co^{II}-derivatized myoglobin, Co^{II}–Mb, was prepared as previously described.[24] All other materials including cystamine [bis-(2-aminoethyl) disulfide] (Aldrich), 1-[(3-dimethylamino)propyl]-3-ethylcarbodiimide (EDC) (Aldrich), microperoxidase-11 (MP-11) (Sigma), myoglobin (from horse heart, Sigma), glutaric dialdehyde (Aldrich) and acetylenedicarboxylic acid (Aldrich) were used without further purification. Ultrapure water from a Nanopure (Braunstead) source was used throughout this work.

Electrode modification

Au electrodes (0.5 mm diameter Au wire, geometrical area *ca.* 0.2 cm^2, roughness factor *ca.* 1.5) were cleaned from deposited monolayers as previously described.[25] Clean Au electrodes were roughened (roughness factor *ca.* 15–20) and modified with a cystamine monolayer as reported previously.[26] The freshly prepared cystamine-modified Au electrodes were used for covalent coupling with microperoxidase-11 (MP-11) in the presence of EDC.[27] MP-11 monolayer-modified Au electrode was incubated in 3.5×10^{-4} M Co^{II}–Mb in 0.1 M phosphate buffer, pH 7.1, for 15 min, rinsed quickly (2 s) with the phosphate buffer and treated with 10% (v/v) glutaric dialdehyde in water for 15 min to

cross-link the adsorbed protein molecules on the electrode surface. A rotating disk electrode (RDE) (4.5 mm diameter) was polished with an alumina suspension (0.3 μm Buehler, IL, USA), rinsed with water and then modified in the same way as Au wire electrodes.

Measurements

Electrochemical measurements (cyclic voltammetry and amperometry under constant applied potential) were performed using a potentiostat (EG&G VersaStat) connected to a personal computer (EG&G research electrochemistry software model 270/250). All the measurements were carried out at ambient room temperature (22 ± 2 °C) in a three compartment electrochemical cell consisting of the chemically modified electrode as a working electrode, a glassy carbon auxiliary electrode isolated by a glass frit and a saturated calomel electrode (SCE) connected to the working volume with a Luggin capillary. All potentials are reported with respect to this reference electrode. Argon bubbling was used to remove oxygen from the solution in the electrochemical cell. Phosphate buffer (0.1 M, pH = 7.1) was used as a background electrolyte. For all constant potential measurements (steady-state current measurements, electrolysis with HPLC detection of maleic acid, RDE measurements) the working electrode potential was −0.5 V. To accumulate the reduced product (maleic acid), a constant potential electrolysis was performed at an integrated MP-11/Co^{II}–Mb monolayer electrode (an Au wire electrode with a geometrical surface area of *ca.* 0.2 cm^2 and a roughness factor of *ca.* 15). The concentration of maleic acid during the electrolysis was determined by HPLC, using a Merck-Hitachi instrument equipped with a Shodex KC-811 ionpack column (0.1% H_3PO_4) and an optical detector (190–370 nm). The RDE measurements were performed with an electrode rotator (model 636, EG&G). The rate of rotation was increased stepwise, and after each step the cathodic current was measured when it had stabilized (after a few seconds).

A quartz crystal microbalance analyzer (QCM) (EG&G model QCA 917) linked to a personal computer, was employed for the microgravimetric analyses. Quartz crystals (AT-cut, EG&G) sandwiched between two Au electrodes ($A = 0.196$ cm^2, roughness factor *ca.* 3.5) were used. The fundamental frequency of the crystals was *ca.* 9.0 MHz. The crystal was mounted in a home-built flow-cell, *ca.* 1 ml, that included an injection septum and permitted *in situ* rinsing of the cell solution with an external peristaltic pump. Modification of the Au–quartz crystal with the MP-11 monolayer was carried out in the same way as for other Au electrodes.

Results and discussion

Microperoxidase-11, MP-11, was assembled on Au electrodes as shown in Scheme 1. The hemopolypeptide was coupled to a base cystamine monolayer associated with the electrode. Fig. 1 shows the cyclic voltammogram of the resulting MP-11 monolayer on a non-roughened Au wire (geometrical area 0.2 cm^2, roughness factor[28] *ca.* 1.5). The inset shows the cyclic voltammogram of the MP-11 monolayer on a rough Au wire-electrode of similar geometrical area (0.2 cm^2, roughness factor *ca.* 15). By coulometric analysis of the reduction (or oxidation) waves, we estimate the surface coverage of MP-11, on the roughened and smooth electrodes, to be 3×10^{-10} mol cm^{-2} and 5×10^{-10} mol cm^{-2}, respectively. These values are consistent with the real surface areas of the respective electrodes. In a recent study,[29] the electron transfer at the MP-11 monolayer was kinetically resolved using chronoamperometry. Two modes of covalent attachment of MP-11 in the monolayer assembly were suggested. One mode involves the linkage of the porphyrin carboxylic function to the monolayer whereas the other mode includes the linkage of the oligopeptide to the monolayer

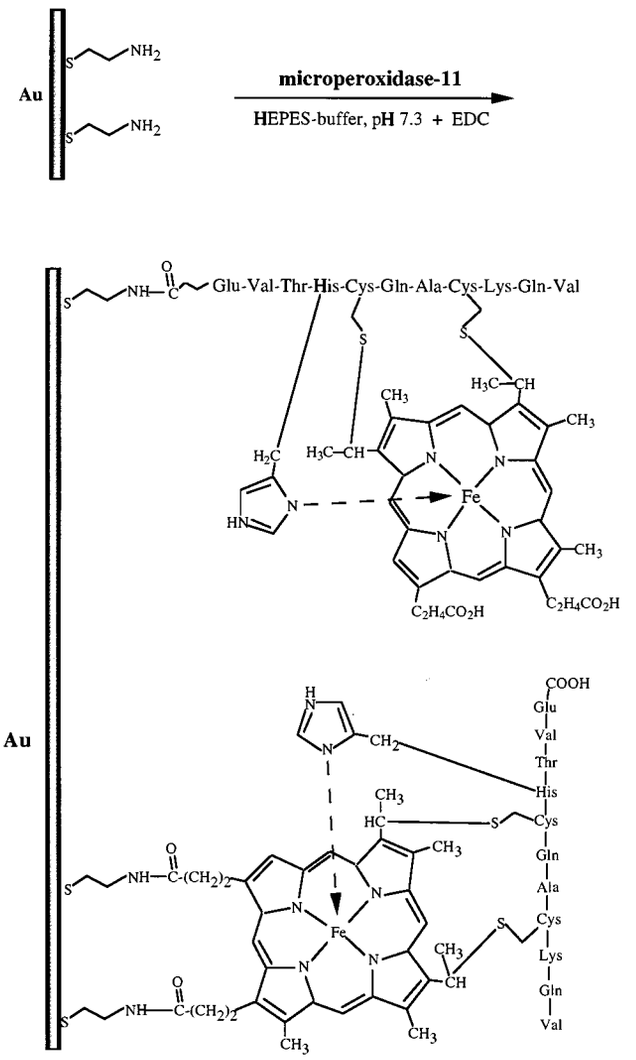

Scheme 1 Stepwise organization of the MP-11 monolayer on an Au electrode

(Scheme 1). The ratio of the respective MP-11 binding modes to the monolayer was estimated to be *ca.* 1 : 1.

Co^{II}–protoporphyrin IX reconstituted myoglobin, Co^{II}–Mb, was prepared as shown in Scheme 2. The Fe^{II}–protoporphyrin

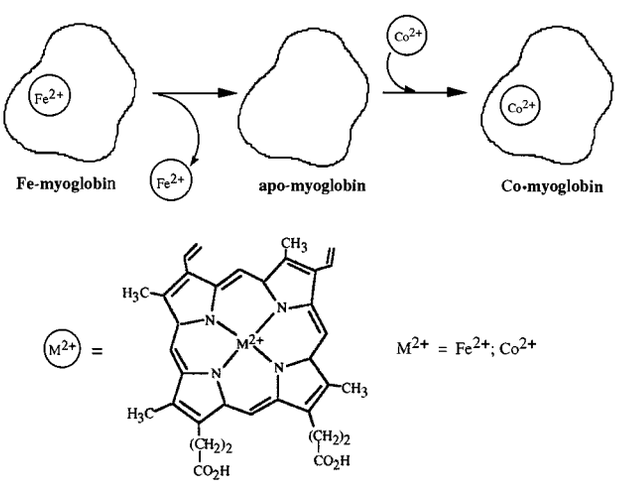

Scheme 2 Formation of apo-myoglobin and its reconstitution with Co^{II}–protoporphyrin IX

was excluded from the hemoprotein and Co^{II}–protoporphyrin IX was introduced into the apo-myoglobin. The formation of Co^{II}–Mb is supported by the appearance of the specific band,

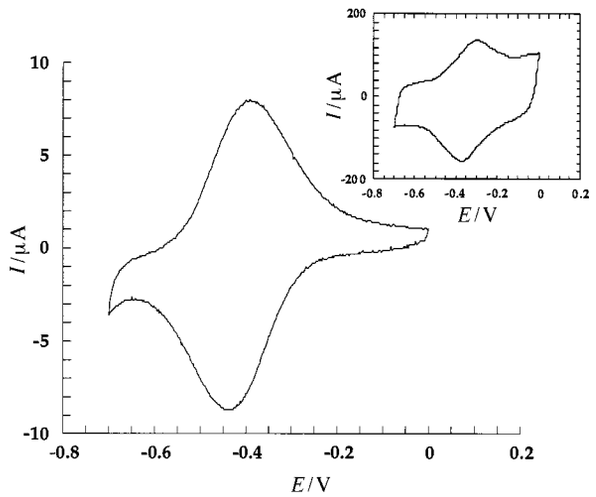

Fig. 1 Cyclic voltammogram of the MP-11 monolayer on a smooth Au electrode (roughness factor *ca.* 1.5); scan rate, 100 mV s^{-1}. Inset: cyclic voltammogram of the MP-11 monolayer on a rough Au electrode (roughness factor 15), scan rate 200 mV s^{-1}. Measurements were taken in 0.1 M phosphate buffer, pH = 7.1.

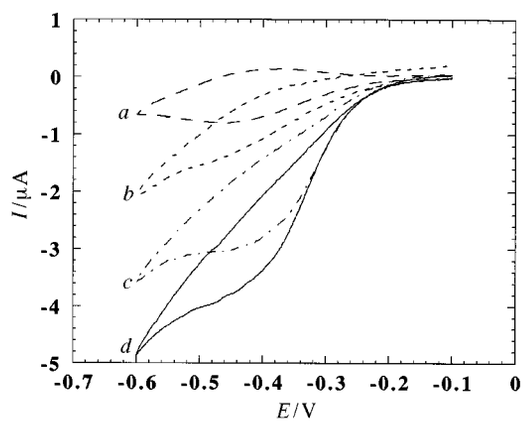

Fig. 2 Cyclic voltammograms of the MP-11 monolayer-modified Au electrode (roughness factor *ca.* 1.5): (*a*) *vs.* background solution: 0.1 M, phosphate buffer, pH = 7.1, (*b*) in the presence of 5×10^{-5} M Co^{II}–Mb, (*c*) in the presence of 5×10^{-5} M Co^{II}–Mb and 50 mM acetylenedicarboxylic acid, (*d*) in the presence of 5×10^{-5} M Co^{II}–Mb and 100 mM acetylenedicarboxylic acid, potential scan rate, 5 mV s^{-1}

$\lambda_{max} = 426$ nm, in the absorbance spectrum.[30] Co^{II}–Mb is by itself electrochemically inactive at bare and cystamine modified Au electrodes.

Fig. 2 shows the cyclic voltammogram of the MP-11 functionalized Au electrode in the presence of added Co^{II}–Mb [Fig. 2(*b*)]. An electrocatalytic cathodic current is observed at the reduction wave of the MP-11 monolayer electrode, implying the MP-11 electrocatalyzed reduction of Co^{II}–Mb. Further mechanistic insight into the MP-11 mediated reduction of Co^{II}–Mb was obtained by the use of a rotating disc electrode, RDE. The MP-11 monolayer was assembled on an Au disc, and the resulting electrocatalytic cathodic currents were determined at different Co^{II}–Mb concentrations and variable rotation speeds upon the application of a constant potential corresponding to −0.5 V on the disc electrode. Fig. 3(*a*) shows the theoretical catalytic current at variable rotation speeds for [Co^{II}–Mb] = 1×10^{-5} M, calculated by application of the Levich equation[31] [eqn. (1)],

$$I_{cat}(A) = 0.62\, nFAD^{2/3}\omega^{1/2}\, \nu^{-1/6}[Co^{II}\text{–Mb}] \qquad (1)$$

where n = number of electrons involved in the electrochemical process; F = Faraday constant; $A = 0.2$ cm^2, real electrode area; $D = 1.1 \times 10^{-6}$ cm^2 s^{-1}, the diffusion coefficient of Mb,[32] $\nu = 0.01$ cm^2 s^{-1}, the kinematic viscosity for water,[31] [Co^{II}–Mb] = Derivatized myoglobin concentration (mol cm^{-3}).

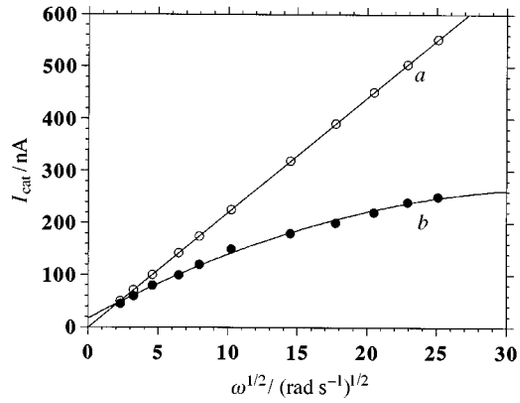

Fig. 3 Electrocatalytic current corresponding to the reduction of Co^{II}–Mb on the MP-11 modified Au rotating disk electrode *vs.* $\omega^{1/2}$; (*a*) theoretical Levich plot corresponding to eqn. (1), (*b*) experimentally measured electrocatalytic currents in the presence of 1×10^{-5} M Co^{II}–Mb. Background solution: 0.1 M phosphate buffer, pH = 7.1; applied potential −0.5 V.

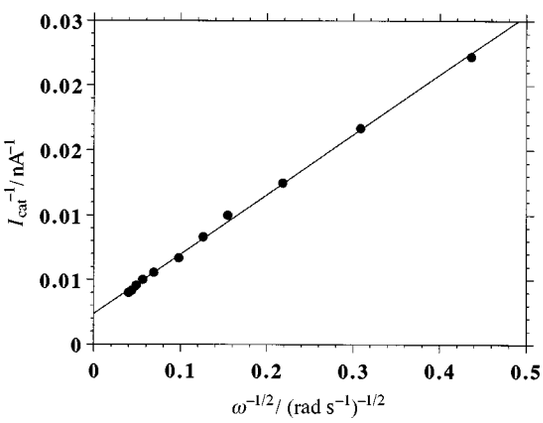

Fig. 4 Koutecky–Levich plot for the system described in Fig. 3(*b*)

Fig. 3(*b*) shows the experimental catalytic currents observed at different rotation speeds, [Co^{II}–Mb] = 1×10^{-5} M. The observed catalytic currents at variable rotation speeds were replotted in terms of the Koutecky–Levich formulation,[31] Fig. 4. From the slope of the linear plot, we determine that MP-11 electrocatalyzed reduction of Co^{II}–Mb involves a single electron transfer ($n = 1$). The interfacial electron transfer rate-constant, k_{el}, was determined from the intercept [eqn. (2)]. For

$$k_{el} = \frac{I(\omega \rightarrow \infty)}{nFA[Co^{II}\text{–Mb}]} \qquad (2)$$

example, for a concentration of Co^{II}–Mb corresponding to 1×10^{-5} M, we derive $k_{el} = 2.75 \times 10^{-3}$ cm s^{-1}. As the MP-11 surface density corresponds to $\Gamma = 1 \times 10^{-10}$ mol cm^{-2}, the overall, second-order, interfacial electron transfer, $k_{overall}$ ($k_{overall} = k_{el}/\Gamma$), corresponds to $k_{overall} = 7 \times 10^3$ M^{-1} s^{-1}. The $k_{overall}$ values were determined for different concentrations of [Co^{II}–Mb], Fig. 5. As the concentration of Co^{II}–Mb increases, $k_{overall}$ decreases, and a linear relationship between $k_{overall}^{-1}$ and Co^{II}–Mb is present. Note that if the electrocatalyzed reduction of Co^{II}–Mb by MP-11 is diffusionally controlled, then the plot $k_{overall}^{-1}$ *vs.* Co^{II}–Mb concentration should be constant (zero slope), since $k_{overall}^{-1}$ is determined at $\omega = \infty$. The non-zero slope of the $k_{overall}^{-1}$ plot, Fig. 5, is indicative of the formation of a complex between the MP-11 monolayer and Co^{II}–Mb [reaction (3)].

$$|\text{–MP-11}_{red} + Co^{II}\text{–Mb} \underset{k_{-1}}{\overset{k_1}{\rightleftharpoons}} |\text{–MP-11}_{red} \cdots Co^{II}\text{–Mb} \xrightarrow{k_{+2}} |\text{–MP-11}_{ox} + Co^{I}\text{–Mb} \qquad (3)$$

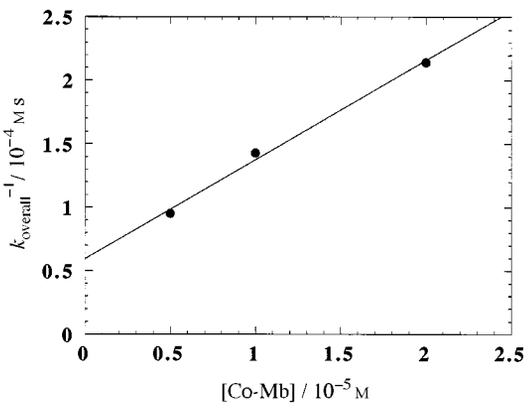

Fig. 5 Second-order rate constants ($k_{overall}$) for the reduction of Co^{II}–Mb at the MP-11 modified-electrode *vs.* the Co^{II}–Mb concentrations

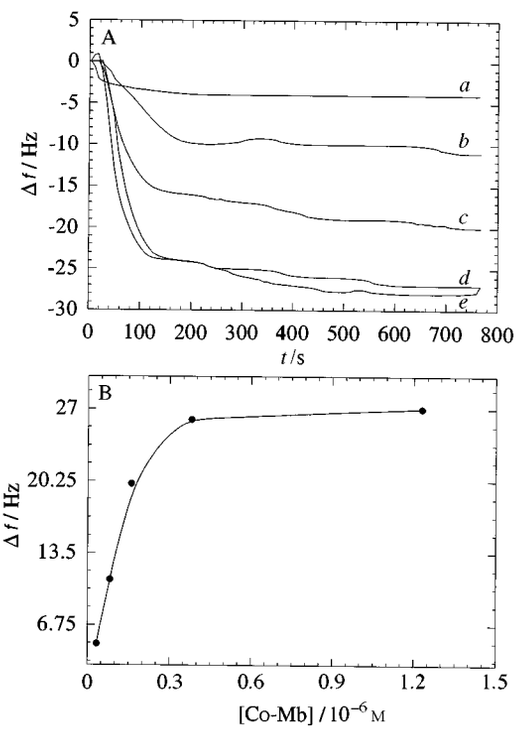

Fig. 6 (A) Time-dependent frequency changes of the MP-11 modified Au–quartz crystal in the presence of different concentrations of Co^{II}–Mb: (*a*) 3.3×10^{-8} M; (*b*) 8.2×10^{-8} M; (*c*) 1.6×10^{-7} M; (*d*) 3.8×10^{-7} M; (*e*) 1.23×10^{-6} M. (B) Steady-state, equilibrated frequency changes of the MP-11 modified Au–quartz crystal at different concentrations of Co^{II}–Mb.

According to this equation, the overall electron transfer rate constant is given by eqn. (4), which can be rearranged in terms of eqn. (5), where K_M is expressed by eqn. (6). From the plot

$$k_{overall} = \frac{k_{+2}}{K_M + [Co^{II}\text{–Mb}]} \quad (4)$$

$$\frac{1}{k_{overall}} = \frac{K_M}{k_{+2}} + \frac{1}{k_{+2}}[Co^{II}\text{–Mb}] \quad (5)$$

$$K_M = \frac{k_{+2}}{k_1 + k_{-1}} \quad (6)$$

shown in Fig. 5, we calculate $k_{+2} = 0.3\ s^{-1}$ and $K_M = 7.8 \times 10^{-6}$ M, respectively. Thus, the RDE experiments indicate that the electrocatalyzed reduction of Co^{II}–Mb by MP-11 occurs by the formation of an intermolecular complex between MP-11 and Co^{II}–Mb, at the monolayer interface, in which the transfer of one electron proceeds.

Further support regarding the formation of the complex between MP-11 and Co^{II}–Mb at the monolayer interface is obtained by microgravimetric, quartz-crystal-microbalance, QCM, experiments. Au electrodes associated with a quartz crystal (AT-cut, 9 MHz), were modified by MP-11 and the crystal frequency changes, Δf, at different Co^{II}–Mb concentrations, were monitored [Fig. 6(A)]. The Δf of the crystal is enhanced. Upon interaction of the MP-11 functionalized crystal with Co^{II}–Mb, a time-dependent decrease in the crystal frequency is observed, reflecting the dynamics of Co^{II}–Mb association to the monolayer. The crystal frequency then levels off to a constant value that represents the steady-state equilibrated condition of the associated Co^{II}–Mb with the monolayer. The change of the crystal frequency, Δf, correlates with the mass change occurring on the crystal due to the binding of Co^{II}–Mb, according to the Sauerbrey equation[33] [eqn. (7)]. Fig. 6(B) shows the equilibrated crystal frequency changes Δf of the crystal at different concentrations of Co^{II}–Mb. The change in frequency reaches a saturation value that suggests that the MP-11 monolayer is saturated with Co^{II}–Mb. The frequency changes occurring on the crystal relate to mass changes, or surface coverage, by the Co^{II}–Mb. The surface coverage of MP-11 on the Au electrodes associated with the crystal, was independently determined by electrochemical means. This allowed us to determine the association constant of Co^{II}–Mb to the MP-11 monolayer, $K_a = 1.6 \times 10^5\ M^{-1}$.

$$\Delta f = -2.3 \times 10^{-6} f_o^2 (\Delta m / A) \quad (7)$$

The MP-11 electrocatalyzed reduction of Co^{II}–Mb yields Co^{I}–Mb. The chemistry of Co^{I} complexes in aqueous media has been extensively characterized and utilized in a variety of photocatalyzed and thermally induced catalytic transformations.[34] In aqueous media, Co^{I} complexes yield Co^{III}–hydride species. Protonation of the resulting hydride to evolve hydrogen is slow, and hence insertion of various substances such as CO_2, acetylenes or N_2 to the reactive hydride species, was observed. This led to electrocatalyzed CO_2-fixation[35] and hydrogenation of acetylene.[36] Accordingly, the MP-11 mediated electrocatalyzed reduction of Co^{II}–Mb was coupled to the two-electron hydrogenation of acetylenedicarboxylic acid, Scheme 3. Fig. 2(*c*) and (*d*) shows the cyclic voltammograms of the MP-11 monolayer electrode in the presence of Co^{II}–Mb upon addition of the substrate, acetylenedicarboxylic acid. Clearly, as the concentration of the substrate increases, the electrocatalytic cathodic current is enhanced. Control experiments reveal that no electrocatalytic cathodic current is observed upon addition of the substrate to the MP-11 functionalized electrode in the absence of Co^{II}–Mb. These results imply that acetylenedicarboxylic acid is reduced by a process catalyzed by Co^{II}–Mb. As we will describe later, the reduction of the substrate corresponds to its hydrogenation to

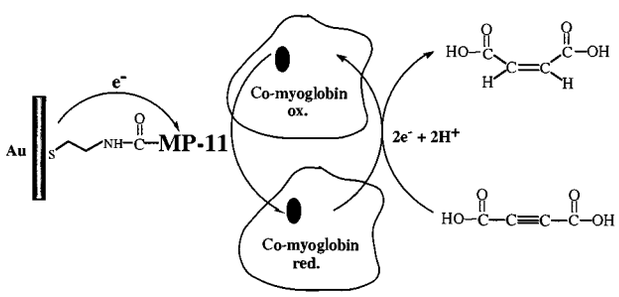

Scheme 3 Co^{II}–Mb mediated hydrogenation of acetylenedicarboxylic acid in the presence of the MP-11 monolayer-functionalized Au electrode

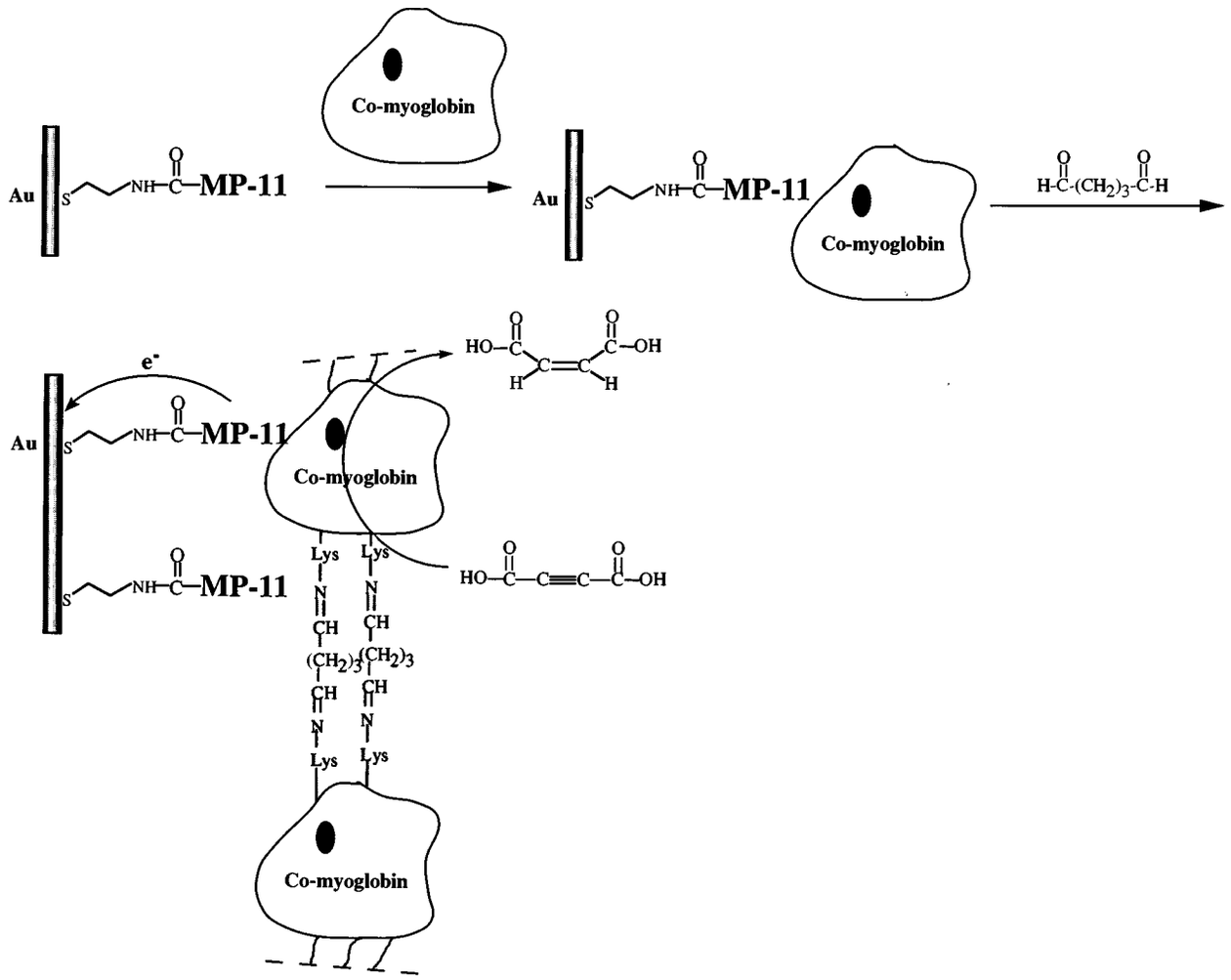

Scheme 4 Stepwise assembly of the integrated MP-11/Co^{II}–Mb monolayer-modified Au electrode and the bioelectrocatalyzed reduction of acetylenedicarboxylic acid at the functionalized electrode

maleic acid, by insertion of the acetylenedicarboxylic acid into the Co^{III}–hydride–Mb species.

The binding of Co^{II}–Mb to the MP-11 monolayer electrode, by affinity associative interactions, leads to a complex in which electrocatalytic reduction of Co^{II}–Mb occurs. Since the complex between Co^{II}–Mb and MP-11 is stable, cross-linking of the Co^{II}–Mb is expected to yield a polymeric Co^{II}–Mb layer of multi-anchoring sites to the electrode support. This is then anticipated to yield an integrated, stable, electrocatalytic electrode for the hydrogenation of acetylenedicarboxylic acid. Scheme 4 shows the assembly of the integrated, cross-linked, electrocatalytic electrode. The electrode obtained by the association of Co^{II}–Mb to the MP-11 monolayer by affinity associative interactions, was cross-linked in the presence of glutaric dialdehyde to generate the cross-linked protein layer. Fig. 7 shows the cyclic voltammograms of the resulting cross-linked MP-11/Co^{II}–Mb electrode in the presence of different concentrations of acetylenedicarboxylic acid. Fig. 8(A) shows the electrocatalytic current of the MP-11/Co^{II}–Mb electrode at different concentrations of the substrate. The current increases as the concentration of acetylenedicarboxylic acid is elevated, and it levels off to an almost constant value at a concentration of the substrate corresponding to *ca.* 100 mM. Such behavior is consistent with an enzyme-like Co^{II}–hydride–Mb catalytic hydrogenation of the substrate, where the saturation of the catalyst leads to a maximal rate in the hydrogenation process.

A tentative mechanism for the electrocatalyzed hydrogenation of acetylene is outlined in Scheme 5. This cycle assumes the participation of the Co^{III}–H as the reactive catalytic species. This cycle follows the formulation of an enzyme catalyzed process, where the formation of a complex with the substrate generates the active assembly for the catalytic transformation. The electrocatalytic currents shown in Fig. 8(A) relate to the rate of the hydrogenation reaction. Thus, the plot can be analyzed by the Michaelis–Menten model [reaction (3)]. The saturation rate, V_{max}, for the electrocatalyzed reduction of Co^{II}–Mb is given by eqn. (8). As the rates of electron transfer at any Co^{II}–Mb concentration are reflected by the electrocatalytic currents, eqn. (8)

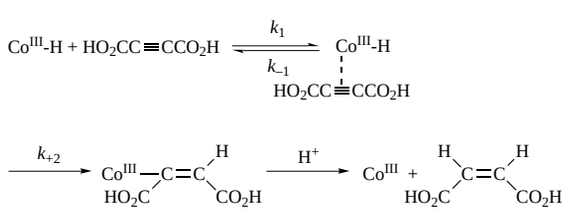

Scheme 5

$$\frac{1}{V}=\frac{1}{V_{max}}+\frac{K_M}{V_{max}[Co^{II}\text{–Mb}]} \quad (8)$$

can be reorganized in terms of eqn. (9), where I_{max} is the satur-

$$\frac{1}{I}=\frac{1}{I_{max}}+\frac{K_M}{I_{max}[Co^{II}\text{–Mb}]} \quad (9)$$

ation current and K_M is given by eqn. (6). Lineweaver–Burk analysis [Fig. 8(B)] of the curve shown in Fig. 8(A) yields the value I_{max} = 5.8 μA and K_M = 90 mM.

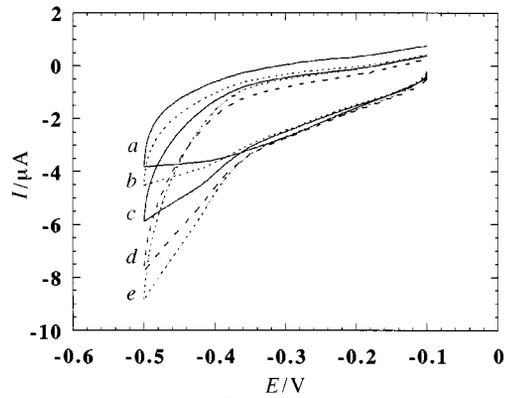

Fig. 7 Cyclic voltammograms of the integrated MP-11/Co^{II}–Mb monolayer-modified Au electrode (roughness factor *ca.* 15): (*a*) *vs.* background solution: 0.1 M phosphate buffer, pH 7.1, (*b*), (*c*), (*d*) and (*e*) in the presence of 8.2, 32, 62 and 76 mM of acetylenedicarboxylic acid, respectively. Potential scan rate, 5 mV s^{-1}.

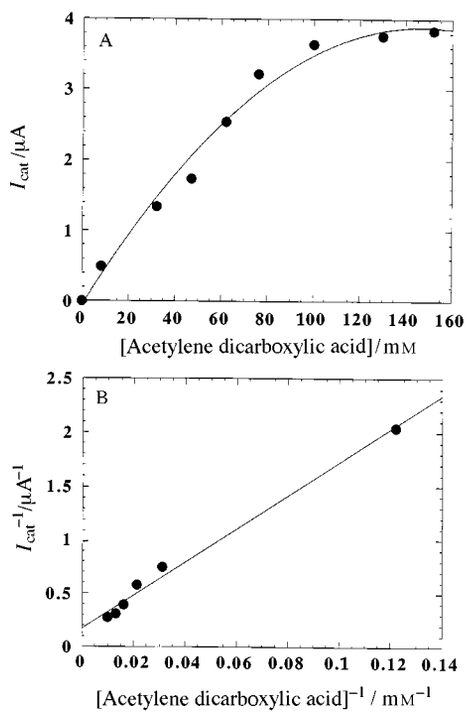

Fig. 8 (A) Electrocatalytic cathodic currents (measured at $E = -0.5$ V in a non-stirred solution) transduced by the integrated MP-11/Co^{II}–Mb electrode (roughness factor 15) at different concentrations of acetylenedicarboxylic acid. Measurements were taken in 0.1 M phosphate buffer, pH = 7.1. (B) Lineweaver–Burk plot for the experimental data shown in Fig. 8(A).

Two aspects related to the electrocatalyzed hydrogenation of acetylenedicarboxylic acid require further investigation. (*i*) It is essential to prove that the electrocatalyzed reduction of acetylenedicarboxylic acid involves the hydrogenation of the substrate and to identify the product. (*ii*) To support the participation of a Co^{III}–H species as a catalytic site for the hydrogenation of the substrate.

The integrated MP-11/Co^{II}–Mb electrode was applied to continuous electrolysis of acetylenedicarboxylic acid upon application of a constant potential of $E = -0.5$ V. Samples of the electrolyte were analyzed at time intervals of electrolysis by HPLC. The only product formed is maleic acid. Fig. 9 shows the rate of maleic acid formation at different electrolysis time intervals. It should be noted that no fumaric acid (the *trans*-ethylenedicarboxylic acid) is formed even as a trace product. Thus, even though maleic acid is the less stable thermodynamic isomer, it is formed preferentially over fumaric acid. Fig. 10(*a*) shows the charge that passed through the electrolyte cell during the electrolysis. The amount (moles) of maleic acid formed during electrolysis and identified by HPLC would cause the passage of charge through the cell given by Fig. 10(*b*). Thus, the current yield for the electrocatalyzed hydrogenation of the substrate is high and corresponds to *ca.* 80%.

Finally, the electrocatalyzed hydrogenation of acetylenedicarboxylic acid was characterized in water and D_2O. Fig. 11(*a*) and (*b*) show the evolution of maleic acid in H_2O and D_2O, respectively, at time intervals of electrolysis. Clearly, the rate of hydrogenation of the substrate reveals an isotope effect $k_H/k_D \approx 2.7$, which is normal for hydrogen transfer in proteins.[37] This is consistent with the formation of the Co^{III}–H intermediate as the reactive species for the insertion of the substrate.

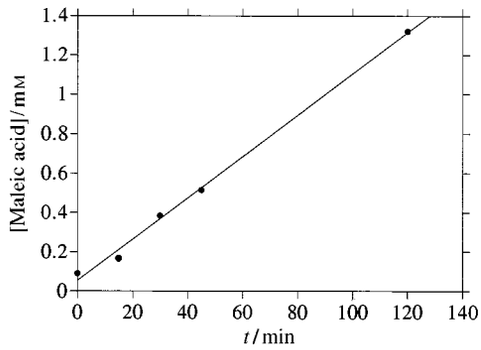

Fig. 9 Rate of maleic acid evolution at time intervals of electrolysis using the integrated MP-11/Co^{II}–Mb monolayer-modified Au electrode (roughness factor *ca.* 15). Electrolysis was carried out at constant potential, −0.5 V, in the presence of acetylenedicarboxylic acid, 76 mM. Background electrolyte: 0.1 M phosphate buffer, pH = 7.1.

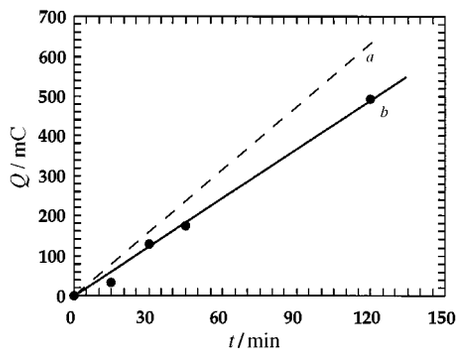

Fig. 10 (*a*) Coulometric analysis of the charge passing the electrolyte cell during hydrogenation of acetylenedicarboxylic acid electrocatalyzed by the MP-11/Co^{II}–Mb integrated electrode. (*b*) Calculated charge that passes the electrolyte cell according to the analyzed hydrogenation product, maleic acid.

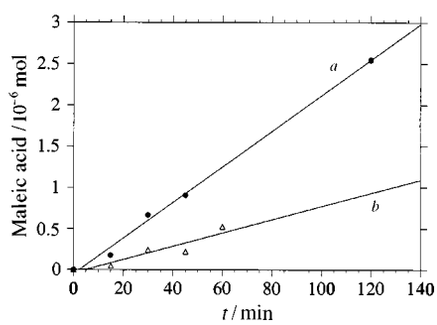

Fig. 11 Rate of maleic acid formation by the integrated MP-11/Co^{II}–Mb electrode in the presence of acetylenedicarboxylic acid, 76 mM, applied potential −0.5 V in: (*a*) H_2O; (*b*) D_2O. In both systems, the electrolyte is 0.1 M phosphate buffer.

Conclusions

The present study has identified the microperoxidase-11 mediated electrocatalyzed reduction of Co^{II}–protoporphyrin IX reconstituted myoglobin, Co^{II}–Mb. Microgravimetric QCM analyses and RDE experiments revealed the formation of a complex between Co^{II}–Mb and the MP-11 monolayer electrode. This leads to the intra-complex electron transfer and the reduction of Co^{II}–Mb. The complex formed by associative affinity interactions reveals temporary stability that allows the cross-linking of the associated Co^{II}–Mb layer with glutaric dialdehyde. The resulting integrated MP-11/Co^{II}–Mb layered electrode reveals high stability and exhibits electrocatalytic properties for the stereospecific electrocatalyzed hydrogenation of acetylenedicarboxylic acid to maleic acid. Electrolysis of the substrate proceeds with a high current yield of *ca.* 80%. The assembly of other integrated MP-11/metal–porphyrin reconstituted protein electrodes by similar affinity associative interactions, to stimulate other electrocatalytic transformations seems feasible.

Acknowledgements

This research was supported by the Deutsche Forschung Gesellschaft (DFG), Germany.

References

1 M. Brunori, *Biosens. Bioelectron.*, 1994, **9**, 633.
2 (*a*) H. A. O. Hill and N. J. Walton, *J. Am. Chem. Soc.*, 1982, **104**, 6515; (*b*) H. A. O. Hill, N. J. Walton and I. J. Higgins, *FEBS Lett.*, 1981, **126**, 282; (*c*) A. E. G. Cass, G. Davis, H. A. O. Hill and D. J. Nancarrow, *Biochim. Biophys. Acta*, 1985, **828**, 51.
3 P. A. Adams, in *Peroxidases in Chemistry and Biology*, ed. J. Everse and K. E. Everse, CRC Press, Boston, vol. 2, ch. 7, p. 171.
4 S. Dong and Q. Chi, *Bioelectrochem. Bioenerg.*, 1992, **29**, 237.
5 I. Taniguchi, H. Kurihara, K. Yoshida, M. Tominaga and F. M. Hawkridge, *Denki Kagaku*, 1992, **60**, 1043.
6 (*a*) F. A. Armstrong, H. A. O. Hill and N. J. Walton, *Q. Rev. Biophys.*, 1968, **18**, 261; (*b*) F. A. Armstrong, H. A. O. Hill and N. J. Walton, *Acc. Chem. Res.*, 1988, **21**, 407; (*c*) J. E. Frew and H. A. O. Hill, *Eur. J. Biochem.*, 1988, **172**, 261.
7 (*a*) P. M. Allen, H. A. O. Hill and N. J. Walton, *J. Electroanal. Chem.*, 1984, **178**, 69; (*b*) I. Taniguchi, K. Toyosawa, H. Yamaguchi and K. Yasukouchi, *J. Chem. Soc., Chem. Commun.*, 1982, 1032.
8 T. Lu, X. Yu, S. Dong, C. Zhou, S. Ye and T. M. Cotton, *J. Electroanal. Chem.*, 1994, **369**, 79.
9 X. Qu, T. Lu, S. Dong, C. Zhou and T. M. Cotton, *Bioelectrochem. Bioenerg.*, 1994, **34**, 153.
10 G. Li, H. Chen and D. Zhu, *Anal. Chim. Acta*, 1996, **319**, 275.
11 (*a*) M. J. Tarlov and E. F. Bowden, *J. Am. Chem. Soc.*, 1991, **113**, 1847; (*b*) D. Hobara, K. Niki, C. Zhou, G. Chumanov and T. M. Cotton, *Colloids Surf. A*, 1994, **93**, 241; (*c*) T. M. Nahir and E. F. Bowden, *J. Electroanal. Chem.*, 1996, **410**, 9.
12 (*a*) F. Scheller, M. Janchen, J. Lampe, H. J. Prümke, J. Blanck and E. Palecek, *Biochim. Biophys. Acta*, 1975, **412**, 157; (*b*) J. F. Stargardt, F. M. Hawkridge and H. L. Landrum, *Anal. Chem.*, 1978, **50**, 930; (*c*) T. M. Cotton, S. G. Schultz and R. P. van Duyne, *J. Am. Chem. Soc.*, 1980, **102**, 7960.
13 M. Tominaga, T. Kumagai, S. Takita and I. Taniguchi, *Chem. Lett.*, 1993, 1771.
14 (*a*) A. C. Onouha and J. F. Rusling, *Langmuir*, 1995, **11**, 3296; (*b*) A.-E. F. Nassar, W. S. Willis and J. F. Rusling, *Anal. Chem.*, 1995, **67**, 2386.
15 G. Li, H. Fang, Y. Qian and H. Chen, *Electroanalysis*, 1996, **8**, 465.
16 (*a*) J. F. Stargardt, F. M. Hawkridge and H. L. Landrum, *Anal. Chem.*, 1978, **50**, 930; (*b*) S. Song and S. Dong, *Bioelectrochem. Bioenerg.*, 1988, **19**, 337.
17 A. Narvaez, E. Dominguez, I. Katakis, E. Katz, K. T. Ranjit, I. Ben-Dov and I. Willner, *J. Electroanal. Chem.*, in the press.
18 E. Zahavy and I. Willner, *J. Am. Chem. Soc.*, 1996, **118**, 12 499.
19 I. Willner, E. Zahavy and V. Heleg-Shabtai, *J. Am. Chem. Soc.*, 1995, **117**, 542.
20 V. Heleg-Shabtai, E. Zahavy and I. Willner, *Energy Convers. Manage.*, 1995, **36**, 609.
21 V. Heleg-Shabtai, E. Katz and I. Willner, *J. Am. Chem. Soc.*, 1997, **119**, 8121.
22 (*a*) I. Willner, E. Katz, B. Willner, R. Blonder, V. Heleg-Shabtai and A. F. Bückmann, *Biosens. Bioelectron.*, 1997, **12**, 337; (*b*) E. Katz, V. Heleg-Shabtai, B. Willner, I. Willner and A. F. Bückmann, *Bioelectrochem. Bioenerg.*, 1997, **42**, 95; (*c*) I. Willner, V. Heleg-Shabtai, R. Blonder, E. Katz, G. Tao, A. F. Bückmann and A. Heller, *J. Am. Chem. Soc.*, 1996, **118**, 10 321.
23 A. Bardea, E. Katz, A. F. Bückmann and I. Willner, *J. Am. Chem. Soc.*, in the press.
24 F. Ascoli, M. Rosaria, R. Fanelli and E. Antonini, in *Methods in Enzymology*, ed. E. Antonini, L. Rossi-Bernardi and E. Chiancone, Academic Press, London, 1981, vol. 76, p. 72.
25 E. Katz and A. A. Solov'ev, *J. Electroanal. Chem.*, 1990, **291**, 171.
26 E. Katz, D. D. Schlereth and H.-L. Schmidt, *J. Electroanal. Chem.*, 1994, **367**, 59.
27 (*a*) T. Lötzbeyer, W. Schuhmann, E. Katz, J. Falter and H.-L. Schmidt, *J. Electroanal. Chem.*, 1994, **377**, 291; (*b*) A. N. J. Moore, E. Katz and I. Willner, *J. Electroanal. Chem.*, 1996, **417**, 189.
28 (*a*) D. A. J. Rand, R. Woods, *J. Electroanal. Chem.*, 1971, **31**, 29; (*b*) B. E. Conway, *Progr. Surf. Sci.*, 1995, **49**, 331.
29 E. Katz and I. Willner, *Langmuir*, 1997, **13**, 3364.
30 T. Yonetani, H. Yamamoto and G. V. Woodrow, *J. Biol. Chem.*, 1974, **249**, 682.
31 A. J. Bard and L. R. Faulkner, *Electrochemical Methods, Fundamentals and Applications*, Wiley, New York, 1980, ch. 8, p. 280.
32 M. Tominaga, T. Kumagai, S. Takita and I. Taniguchi, *Chem. Lett.*, 1993, 1771.
33 D. A. Buttry, in *Electroanalytical Chemistry*, ed. A. J. Bard, Marcel Dekker, New York, 1991, vol. 17, p. 1.
34 (*a*) J. M. Lehn and R. Ziessel, *Proc. Natl. Acad. Sci. USA*, 1982, **79**, 701; (*b*) F. R. Keene, C. Creutz and N. Sutin, *Coord. Chem. Rev.*, 1985, **64**, 247; (*c*) C. Creutz, N. Sutin, *Coord. Chem. Rev.*, 1981, **64**, 321.
35 (*a*) A. H. A. Tinnemans, T. P. M. Koster, D. H. M. W. Thewissen and A. Mackor, *Recl. Trav. Chim. Pays-Bas*, 1984, **103**, 288; (*b*) D. J. Darensbourg and R. A. Kudaroski, in *Advances in Organometallic Chemistry*, ed. F. G. A. Stone and R. West, Academic Press, New York, 1983, vol. 22, p. 129.
36 E. B. Fleischer and M. Krishnamurthy, *J. Am. Chem. Soc.*, 1972, **94**, 1382.
37 L. I. Krishtalik, *Charge Transfer Reactions in Electrochemical and Chemical Processes*, Consultants Bureau, New York, 1986.

Paper 7/04711H
Received 3rd *July* 1997
Accepted 28*th August* 1997